

The *Arabidopsis* Phosphatidylinositol Phosphate 5-Kinase PIP5K3 Is a Key Regulator of Root Hair Tip Growth ^{WJ|OA}

Hiroaki Kusano,^a Christa Testerink,^b Joop E.M. Vermeer,^b Tomohiko Tsuge,^a Hiroaki Shimada,^c Atsuhiko Oka,^a Teun Munnik,^b and Takashi Aoyama^{a,1}

^a Institute for Chemical Research, Kyoto University, Uji, Kyoto 611-0011, Japan

^b Section of Plant Physiology, Swammerdam Institute for Life Science, University of Amsterdam, 1098 SM Amsterdam, The Netherlands

^c Department of Biological Science and Technology, Tokyo University of Science, Noda, Chiba 278-8510, Japan

Phosphatidylinositol 4,5-bisphosphate [PtdIns(4,5)P₂] functions as a site-specific signal on membranes to promote cytoskeletal reorganization and membrane trafficking. Localization of PtdIns(4,5)P₂ to apices of growing root hairs and pollen tubes suggests that it plays an important role in tip growth. However, its regulation and mode of action remain unclear. We found that *Arabidopsis thaliana* PIP5K3 (for Phosphatidylinositol Phosphate 5-Kinase 3) encodes a phosphatidylinositol 4-phosphate 5-kinase, a key enzyme producing PtdIns(4,5)P₂, that is preferentially expressed in growing root hairs. T-DNA insertion mutations that substantially reduced the expression of PIP5K3 caused significantly shorter root hairs than in the wild type. By contrast, overexpression caused longer root hairs and multiple protruding sites on a single trichoblast. A yellow fluorescent protein (YFP) fusion of PIP5K3, driven by the PIP5K3 promoter, complemented the short-root-hair phenotype. PIP5K3-YFP localized to the plasma membrane and cytoplasmic space of elongating root hair apices, to growing root hair bulges, and, notably, to sites about to form root hair bulges. The signal was greatest in rapidly growing root hairs and quickly disappeared when elongation ceased. These results provide evidence that PIP5K3 is involved in localizing PtdIns(4,5)P₂ to the elongating root hair apex and is a key regulator of the machinery that initiates and promotes root hair tip growth.

INTRODUCTION

Plant cells differentiate into diverse shapes to fulfill their functional requirements. To understand the regulatory mechanisms that give the shape of plant cells, root hairs have been intensively studied as a model system since they are nonessential under experimental growth conditions and highly accessible for microscopic observation (for reviews, see Peterson and Farquhar, 1996; Ridge and Emons, 2000). Root hairs are cellular protuberances resulting from the polar outgrowth of specific root epidermal cells, called trichoblasts. During their morphogenesis, a bulge is initially formed at the distal end on the outer surface of a trichoblast, and the bulge then further protrudes perpendicular to the root surface through highly polarized cell expansion, resulting in a thin cylindrical structure (for reviews, see Gilroy and Jones, 2000; Ryan et al., 2001). This type of cell expansion is called tip growth, because cell growth events, including synthesis of the plasma membrane and cell wall, are limited to the tip. Normally, root hairs are straight and have no branches, indicating that the polarity of root hair tip growth is sustained by a strict regulatory mechanism. The molecular basis of this mechanism is still unclear.

In growing root hairs, cytoskeletal reorganization and vesicular trafficking, both of which are involved in the deposition of materials for the expanding plasma membrane and cell wall, are highly localized to the apical region, and a tip-focused cytoplasmic calcium ion gradient ensures their localization (for reviews, see Hepler et al., 2001; Smith and Oppenheimer, 2005; Cole and Fowler, 2006). Establishment of this calcium ion gradient requires reactive oxygen species, which are generated by the NADPH oxidase ROOT HAIR DEFECTIVE2 in *Arabidopsis thaliana* (Foreman et al., 2003). Recently, the *Arabidopsis* Rho GDP dissociation inhibitor SUPERCENTIPEDE1 (SCN1) was identified as a regulatory component of reactive oxygen species accumulation (Carol et al., 2005). Another line of evidence has revealed that *Arabidopsis* Rho-related GTPases of plants (ROPs) are involved in regulating root hair tip growth as well as bulge initiation (Molendijk et al., 2001; Jones et al., 2002). These results suggest a signal pathway from ROPs leading to the calcium ion gradient via reactive oxygen species accumulation (Carol and Dolan, 2006).

Phospholipid signaling is another important factor for regulating root hair tip growth (for reviews, see Meijer and Munnik, 2003; Fischer et al., 2004; Zonia and Munnik, 2006). Phospholipids function as site-specific signals on membranes and thus are considered to play a pivotal role in localizing intracellular events, such as cytoskeletal reorganization and membrane traffic, to specific loci (for reviews, see van Leeuwen et al., 2004; Di Paolo and De Camilli, 2006; Wang et al., 2006; Krauss and Haucke, 2007; Oude Weernink et al., 2007). Phosphatidic acid (PA) is involved in root hair development, based on the finding that the

¹ Address correspondence to aoyama@scl.kyoto-u.ac.jp.

The author responsible for distribution of materials integral to the findings presented in this article in accordance with the policy described in the Instructions for Authors (www.plantcell.org) is: Takashi Aoyama (aoyama@scl.kyoto-u.ac.jp).

^{WJ} Online version contains Web-only data.

^{OA} Open Access articles can be viewed online without a subscription. www.plantcell.org/cgi/doi/10.1105/tpc.107.056119

Arabidopsis phospholipase D $\zeta 1$ (PLD $\zeta 1$), an enzyme producing PA, is expressed in developing root hair cells, and its ectopic overexpression causes branched root hairs as well as root hairs from atrichoblasts, which are normally hairless cells in the root epidermis (Ohashi et al., 2003). Supporting this idea, a knockout mutation of the *Arabidopsis* *AGC2-1* gene, which encodes an AGC protein kinase acting downstream of PA, confers a short-

root-hair phenotype (Anthony et al., 2004). Green fluorescent protein (GFP) fusions of PLD $\zeta 1$ and AGC2-1 localize to the apical region of growing root hairs (Ohashi et al., 2003; Anthony et al., 2004). Although the localization pattern of PA in root hairs is unknown, it possibly plays a signaling role by recruiting regulatory proteins to specific loci, as seen in animal cells (Munnik, 2001; Testerink and Munnik, 2005).

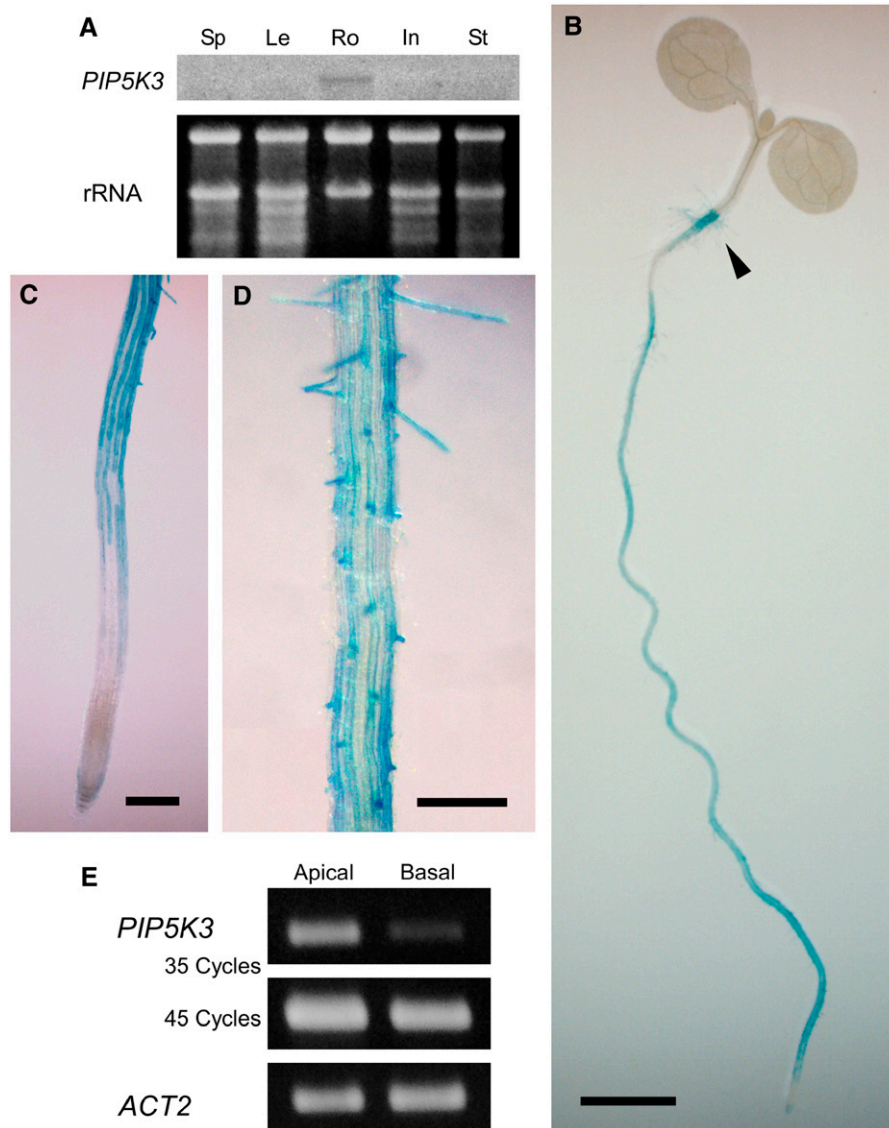


Figure 1. Expression Analyses of *PIP5K3*.

(A) RNA gel blot analysis for organ-specific *PIP5K3* expression. Transcript levels of the *PIP5K3* gene were examined by RNA gel blot analysis using total RNA prepared from seedpods and pollinated flowers (Sp), rosette leaves (Le), roots (Ro), inflorescences without pollinated flowers (In), and stems (St). The same RNA preparations, electrophoresed on an agarose gel and stained with ethidium bromide, are shown below the autoradiogram. Results of the RNA gel blot analysis for other *PIP5K* genes, using the same RNA preparations, are shown in Supplemental Figure 1 online.

(B) to (D) Histochemical analysis of *PIP5K3* promoter activity. Promoter activity of a 1.2-kb DNA fragment upstream of the *PIP5K3* coding region was histochemically analyzed using a GUS reporter gene. The transit region is indicated by an arrowhead in **(B)**. Bars = 2 mm in **(B)** and 0.2 mm in **(C)** and **(D)**.

(E) RT-PCR analysis of *PIP5K3* transcript levels in apical and basal root parts of wild-type plants. *PIP5K3* cDNA amplified with 35 and 45 PCR cycles and positive control cDNA (*ACT2*) amplified with 24 PCR cycles were electrophoresed on agarose gels and stained with ethidium bromide. Three biological replicates showed the same result.

Phosphatidylinositol 4,5-bisphosphate [PtdIns(4,5)P₂], another well-studied signaling phospholipid, regulates signal transduction for not only total cellular responses but also intracellular localizing events in animals and yeast (for reviews, see Downes et al., 2005; van Leeuwen et al., 2004, 2007; Niggli, 2005; Di Paolo and De Camilli, 2006; Krauss and Haucke, 2007). It modulates the functions of a variety of actin regulatory proteins (Yin and Janmey, 2003; Logan and Mandato, 2006) and regulators of exocytotic machinery on the plasma membrane (Olsen et al., 2003; Grishanin et al., 2004; Aoyagi et al., 2005; Li et al., 2006) by directly interacting with its protein targets. In many cases, PtdIns(4,5)P₂ signaling pathways are tightly connected to those of small GTPases belonging to the Rho and Arf families in their upstream and downstream cascades (Santarius et al., 2006). Hence, PtdIns(4,5)P₂ is also expected to play a pivotal regulatory role in the polarized expansion of plant cells. Indeed, PtdIns(4,5)P₂ localizes to the apical plasma membrane and cytoplasmic space of not only root hairs (Braun et al., 1999; Vincent et al., 2005; van Leeuwen et al., 2007) but also pollen tubes (Kost et al., 1999; Dowd et al., 2006; Helling et al., 2006), another tip-growing cellular structure in plants. Moreover, the following evidence suggests that the phosphoinositide metabolic pathway leading to the production of PtdIns(4,5)P₂ is essential for appropriate root hair development. First, a loss of function of the *Arabidopsis* PtdIns binding protein CAN OF WORMS1/SEC FOURTEEN HOMOLOGS1 (COW1/SFH1) compromises both the tip-focused PtdIns(4,5)P₂ and root hair tip growth (Bohme et al., 2004; Vincent et al., 2005). Second, *Arabidopsis* mutant plants with defects in both the *PI-4Kβ1* and *PI-4Kβ2* genes, which encode phosphatidylinositol 4-kinases that produce PtdIns4P from PtdIns, exhibit aberrant root hair morphologies (Preuss et al., 2006).

Despite the general importance of PtdIns(4,5)P₂ in cell morphogenesis and evidence supporting its involvement in root hair development, it is unclear which aspect of root hair development PtdIns(4,5)P₂ regulates and how it is localized to the root hair apex. To address these questions, we focused on Phosphatidylinositol Phosphate 5-Kinase (PIP5K), a key enzyme for the production of PtdIns(4,5)P₂ (Oude Weernink et al., 2004). The *Arabidopsis* genome contains 11 genes encoding proteins with significant sequence similarity to animal PIP5Ks (type I PtdInsP kinases) (Mueller-Roeber and Pical, 2002). These are classified into two subfamilies: proteins of subfamily A (PIP5K10 and PIP5K11) consist of dimerization and catalytic domains similar to those in the animal enzymes, while subfamily B proteins (PIP5K1 to PIP5K9) have an additional domain containing a repeat of the membrane occupation and recognition nexus motif (MORN motif) (Takeshima et al., 2000) at the N terminus. Currently, the biological functions of only *PIP5K1*, *PIP5K4*, and *PIP5K9* have been elucidated as being involved in abscisic acid signaling, stomata opening, and sugar signaling, respectively (Mikami et al., 1998; Lee et al., 2007; Lou et al., 2007). A genome-wide analysis has defined 606 *Arabidopsis* genes as the root hair morphogenesis transcriptome (Jones et al., 2006). However, they do not include any putative PIP5K genes.

In this study, we found that *PIP5K3* encodes the enzyme activity producing PtdIns(4,5)P₂ and is expressed preferentially in root hair cells. T-DNA insertion mutants in which *PIP5K3*

expression levels were substantially reduced had significantly shorter root hairs than did the wild type. Reciprocally, ectopic overexpression of *PIP5K3* caused longer root hairs as well as multiple protruding sites in a single trichoblast. A yellow fluorescent protein (YFP) fusion of PIP5K3 complemented the short-root-hair phenotype, and the fluorescence signal localized not only to the elongating root hair apex but also to the site of future bulge formation on a trichoblast. Our results indicate that PIP5K3 is involved in the spatiotemporal pattern of PtdIns(4,5)P₂ in root hair cells and acts as a key regulatory component of the machinery initiating and promoting root hair tip growth.

RESULTS

The *PIP5K3* Gene Is Expressed in Developing Root Hair Cells

To identify the gene responsible for the production of PtdIns(4,5)P₂ in root hair cells, we first used RNA gel blot analysis to examine the organ-specific expression patterns of the 11 *Arabidopsis* genes encoding putative PIP5Ks. Of the 11 genes, only *PIP5K3* (gene locus, At2g26420) was expressed exclusively in roots (Figure 1A; see Supplemental Figure 1 online). To investigate the expression pattern of *PIP5K3* in more detail, its promoter activity was histochemically examined using an *Escherichia coli* β-glucuronidase (GUS) reporter gene. Consistent with the result of RNA gel blot analysis, a DNA fragment encompassing the 1.2-kb region upstream from the *PIP5K3* initiation codon showed promoter activity in roots and the transit region, or root-hypocotyl junction, where long root hairs develop (Figure 1B). In roots, strong and moderate GUS staining was observed in the cell differentiation zone and more proximal regions, respectively, whereas more distal regions, including the

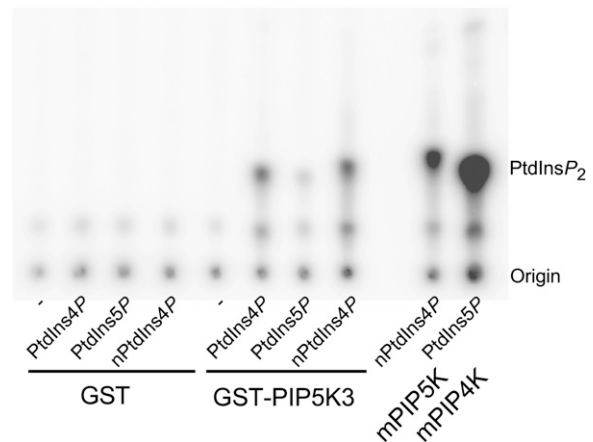


Figure 2. Analysis of PtdInsP Kinase Activity of PIP5K3 in Vitro.

Purified GST-PIP5K3 protein or GST alone was tested for PtdInsP kinase activity on different lipid mixtures containing no lipids (–), synthetic diC16:0 PtdIns4P, synthetic diC16:0 PtdIns5P, or natural PtdIns4P (from brain; nPtdIns4P) in the presence of [γ -³²P]ATP. As positive controls, mammalian type I (mPIP5K) or type II (mPIP4K) PtdInsP kinases were used. The position of PtdIns(4,5)P₂ and the origin are marked.

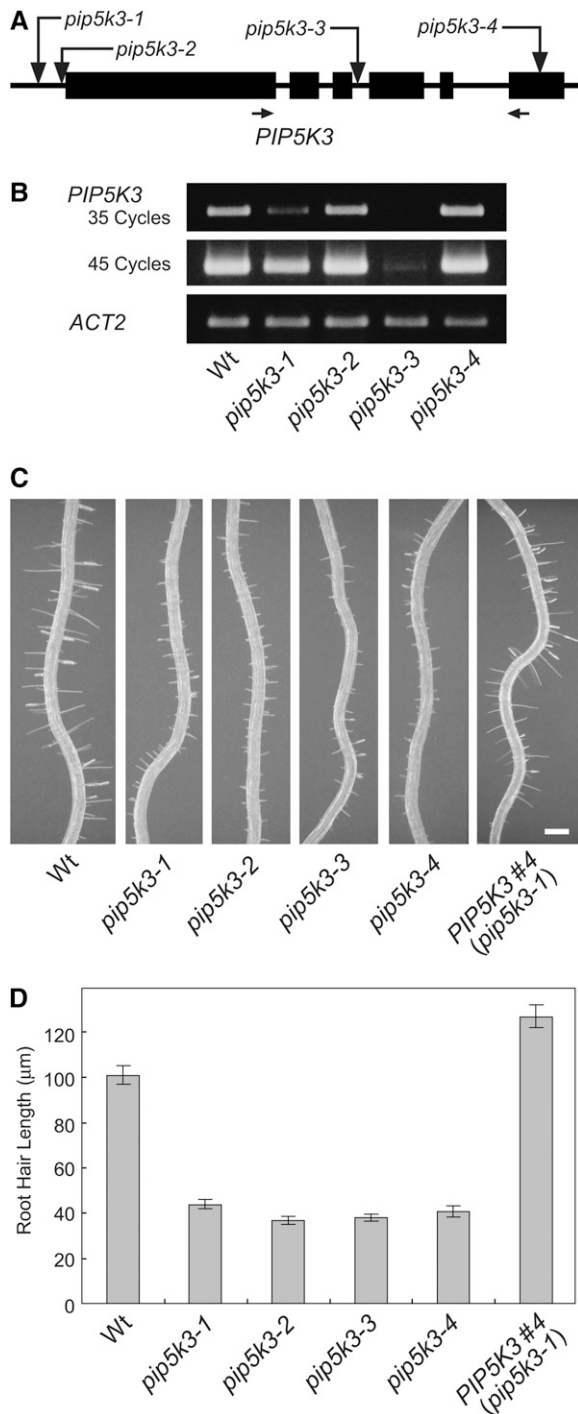


Figure 3. Analyses of T-DNA Insertion Mutants of *PIP5K3*.

(A) Location of T-DNA insertions. The structure of *PIP5K3* is shown schematically, with coding (boxes) and noncoding (lines) regions. Vertical arrows indicate the sites of T-DNA insertions in the mutant lines. Horizontal arrows indicate the positions of the primers used in the RT-PCR analysis.

(B) RT-PCR analysis of T-DNA insertion mutants. *PIP5K3* transcripts were screened for in roots of the wild type and mutant lines. *PIP5K3* cDNA amplified with 35 and 45 PCR cycles and positive control cDNA

meristematic and elongation zones, were only weakly stained (Figure 1C) (for zone definitions, see Dolan et al., 1993). Interestingly, in the cell differential zone and more proximal regions, GUS activity was most pronounced in the root hair cell files (Figures 1C and 1D). To examine the temporal expression pattern of the *PIP5K3* gene further, RT-PCR analysis was performed using total RNA prepared separately from basal root parts, which do not contain developing root hair cells, and apical root parts, which do contain developing root hair cells. As shown in Figure 1E, while transcripts were detected in both parts, the steady state levels of *PIP5K3* transcripts were higher in the apical part than in the basal part. Although this result essentially concurs with that of the GUS reporter analysis, the difference between the two parts was more apparent in the RT-PCR analysis. These results suggest that the *PIP5K3* gene is preferentially active in developing root hair cells.

Recombinant PIP5K3 Protein Shows PtdIns4P 5-Kinase Activity in Vitro

PIP5K3 was expected to have PtdIns4P 5-kinase activity because of its amino acid sequence similarity to *PIP5K1* and *PIP5K4*, for which enzyme activity has been determined in vitro (Mikami et al., 1998; Elge et al., 2001; Westergren et al., 2001; Perera et al., 2005; Lee et al., 2007). To investigate the activity of *PIP5K3*, a fusion protein with glutathione *S*-transferase (GST) was expressed in *E. coli* cells. The fusion protein (GST-*PIP5K3*) was partially purified with glutathione-conjugated beads and subjected to a phosphoinositide kinase assay, using [γ - 32 P]ATP and the two different PtdInsP isomers, PtdIns4P and PtdIns5P, as substrates. Mammalian type I and type II PtdInsP kinases, which produce PtdIns(4,5) P_2 from PtdIns4P and PtdIns5P, respectively, were used as positive controls. As shown in Figure 2, GST-*PIP5K3* produced PtdIns(4,5) P_2 by phosphorylating PtdIns4P, both the natural and synthetic forms. It also phosphorylated PtdIns5P, but less efficiently. These results demonstrate that *PIP5K3* catalyzes the synthesis of PtdIns(4,5) P_2 preferentially from PtdIns4P in vitro.

T-DNA Insertion Mutants of the *PIP5K3* Gene Exhibit a Short-Root-Hair Phenotype

To investigate the function of the *PIP5K3* gene in root hair development, we identified T-DNA insertion lines with defects in the expression of *PIP5K3*. Four SALK lines (Alonso et al., 2003)

(*ACT2*) amplified with 20 PCR cycles were electrophoresed on agarose gels and stained with ethidium bromide. Three biological replicates showed the same result.

(C) and **(D)** Root hair phenotype of T-DNA insertion mutants. Primary roots of the wild type, mutant lines, and the complementation line (*PIP5K3* #4) grown on vertical standing 2% agar medium for 7 d after germination are shown in **(C)**. Bar = 0.2 mm. Lengths of root hairs on the primary root surface were measured, and the means and SE are indicated by the gray bars and error bars ($n > 200$), respectively, in **(D)**. Histograms showing the distributions are provided in Supplemental Figure 3 online.

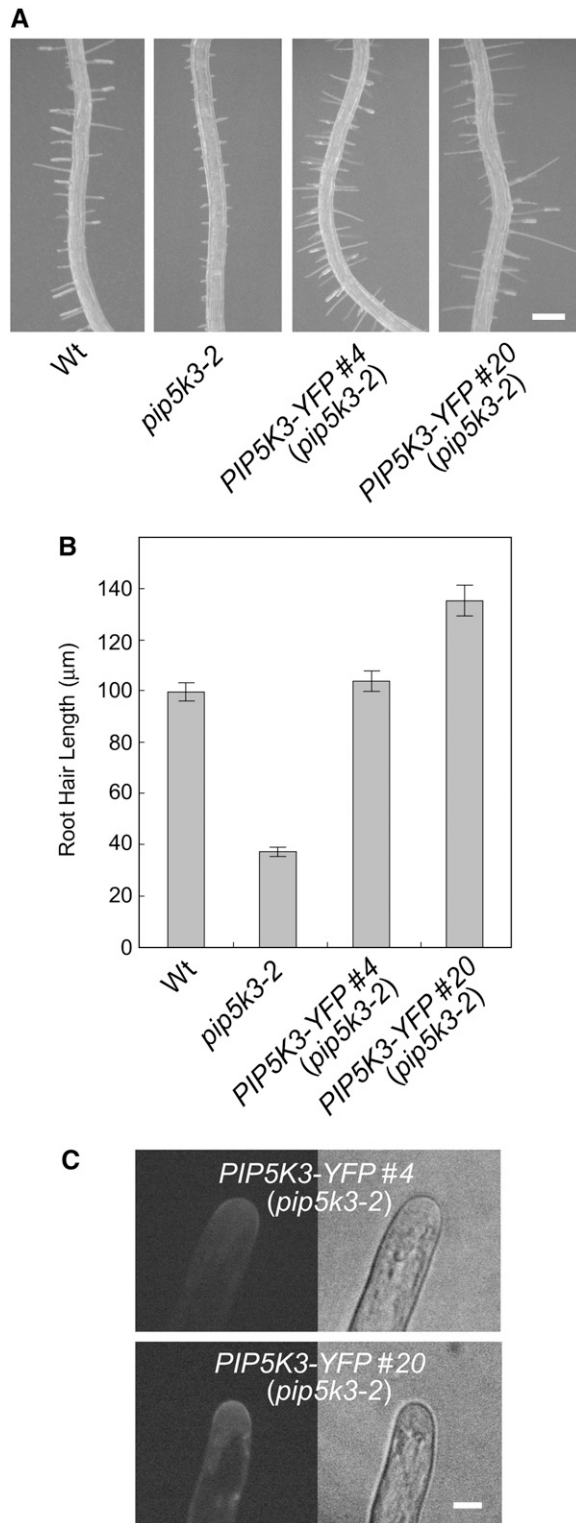


Figure 4. Mutant Complementation by *PIP5K3-YFP*.

(A) and **(B)** Root hair phenotype complemented by *PIP5K3-YFP*. Primary roots of the wild type, the mutant line *pip5k3-2*, and complementation lines with the *pip5k3-2* background (*PIP5K3-YFP* #4 and *PIP5K3-YFP* #20) grown on vertical standing 2% agar medium for 7 d after germina-

tion are shown in **(A)**. Bar = 0.2 mm. Lengths of root hairs on the primary root surface were measured, and the means and SE are indicated by the gray bars and error bars ($n > 200$), respectively, in **(B)**. Histograms showing the distributions are provided in Supplemental Figure 3 online. **(C)** The fluorescence of *PIP5K3-YFP* localized to root hair apices of complementation lines. Apices of vigorously elongating root hairs were observed by confocal laser scanning microscopy. Bar = 10 μm.

that have T-DNA insertions in a region encompassing the *PIP5K3* gene were obtained from the ABRC. Sequencing analysis of the T-DNA borders revealed that SALK_001546 (*pip5k3-1*) and SALK_060590 (*pip5k3-2*) have T-DNA insertions at 152 and 20 bp upstream of the *PIP5K3* initiation codon, respectively, and that SALK_000024 (*pip5k3-3*) and SALK_026683 (*pip5k3-4*) have insertions at 27 bp downstream of the start of the third intron and at 187 bp downstream of the start of the last coding exon, respectively (Figure 3A). In RT-PCR analysis, using total RNA prepared from roots, transcripts encoding a middle part of the *PIP5K3* catalytic domain were detected, but at substantially reduced levels, in homozygous plants of two of the four insertion lines, *pip5k3-1* and *pip5k3-3* (Figure 3B), indicating that these mutations are severely hypomorphic. For the other two lines, *pip5k3-2* and *pip5k3-4*, transcripts were detected at levels similar to those of the wild type (Figure 3B). To determine whether these mutant transcripts can direct functional *PIP5K3* protein production, their sequence structures were determined. For *pip5k3-2*, RT-PCR using various primer sets detected no transcripts containing the authentic 5' untranslated region, but it did detect transcripts with a 5' extension exceeding 1000 nucleotides originating from the T-DNA region (see Supplemental Figure 2 online). In the 5' extension, many ATG and termination codons appear in each frame, suggesting that the translation of *PIP5K3* from the authentic initiation codon is severely affected in *pip5k3-2*. For *pip5k3-4*, RT-PCR detected two splicing variants, in which the sequences encoding the C-terminal 41 and 54 amino acids were lost due to the T-DNA insertion (see Supplemental Figure 2 online). Since the C-terminal regions are highly conserved among the 11 putative *PIP5Ks*, the mutant proteins are thought to have a defect in their molecular function. Thus, all four of the mutant alleles possibly have defects in the expression of the functional *PIP5K3* protein.

None of the mutant lines showed phenotypic changes in their aerial parts (data not shown), which is consistent with the results of the expression analyses. In roots, however, all of the mutant lines exhibited shorter root hairs than the wild type (Figures 3C and 3D; see Supplemental Figure 3 online), indicating the involvement of *PIP5K3* in root hair elongation. With regard to morphology other than the length of root hairs, the root hair cells of all mutant lines appeared normal (e.g., *pip5k3-4* in Supplemental Figure 4 online). Since phenotypic changes in the four alleles were almost identical, it is thought that the production of functional *PIP5K3* was similarly affected in all of the mutant lines. The short-root-hair phenotype was complemented by the expression of a transgene comprising the coding region of *PIP5K3* cDNA driven by the *PIP5K3* promoter (Figures 3C and 3D; see Supplemental Figure 3 online). This confirms that the reduced

tion are shown in **(A)**. Bar = 0.2 mm. Lengths of root hairs on the primary root surface were measured, and the means and SE are indicated by the gray bars and error bars ($n > 200$), respectively, in **(B)**. Histograms showing the distributions are provided in Supplemental Figure 3 online. **(C)** The fluorescence of *PIP5K3-YFP* localized to root hair apices of complementation lines. Apices of vigorously elongating root hairs were observed by confocal laser scanning microscopy. Bar = 10 μm.

expression of functional PIP5K3 is responsible for the short-root-hair phenotype.

PIP5K3-YFP Complemented the *pip5k3* Mutant Defect, and the Signal Localized to the Elongating Root Hair Apex and the Future Bulge Formation Site

To investigate the intracellular localization pattern of PIP5K3, we constructed a chimeric gene comprising the *PIP5K3* promoter and a fragment encoding PIP5K3 with YFP fused to its C terminus (PIP5K3-YFP). The fusion protein gene could complement the short-root-hair phenotype (Figures 4A and 4B; see Supplemental Figure 3 online) in the same way as the gene comprising the *PIP5K3* promoter and the PIP5K3-coding fragment (Figures 3C and 3D). This indicates that PIP5K3-YFP has the same function as PIP5K3 in root hair elongation and, hence, that PIP5K3-YFP very likely undergoes the same posttranslational regulation, including the regulation of intracellular localization and protein degradation, as the authentic PIP5K3 protein. Among the PIP5K3-YFP lines, those expressing the fusion protein at higher levels, as estimated from the intensity of the YFP

fluorescence in elongating root hairs, tended to have longer root hairs (Figures 4B and 4C), suggesting that the amount of PIP5K3 in root hairs is a rate-limiting factor for root hair elongation.

The PIP5K3-YFP localization pattern was analyzed using confocal laser scanning microscopy. YFP fluorescence was predominantly localized to apices of rapidly elongating root hairs but was also detected at relatively low levels in more distal regions of the roots, including the meristematic and elongation zones (Figure 5A). Little YFP fluorescence was detected in more proximal regions containing mature root hairs (Figure 5A). In the apices of elongating root hairs, fluorescence was strongly localized to the plasma membrane and moderately to the cytoplasmic space just below (Figures 5D to 5G; see Supplemental Movie 1 online). To confirm the localization to the plasma membrane, an elongating root hair was treated with a lipophilic fluorescent dye, *N*-(3-triethylammoniumpropyl)-4-(6-(4-(diethylamino)phenyl)hexatrienyl)pyridinium dibromide (FM4-64), for a sufficiently short period that allowed the dye to stain mainly the plasma membrane, and then fluorescence from YFP and FM4-64 was observed simultaneously. The overlay image and scanning patterns of the fluorescence intensities indicated that the YFP

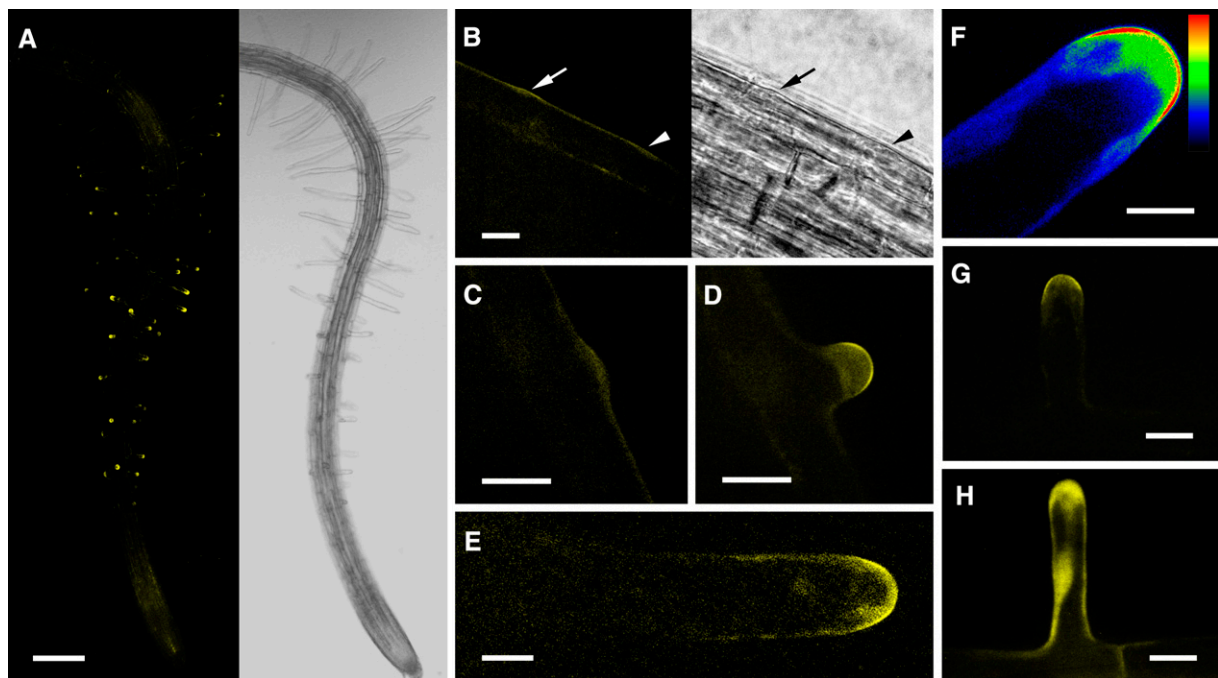


Figure 5. Localization of the Fluorescence Signal in *PIP5K3-YFP* and *PIP5K3ΔM-YFP* Root Hair Cells.

The YFP fluorescence in root hairs expressing *PIP5K3-YFP* and *PIP5K3ΔM-YFP* under the control of the *PIP5K3* promoter was observed using confocal laser scanning microscopy.

(A) A three-dimensional reconstructed fluorescence image (left) and a light image (right) of a *PIP5K3-YFP* root at 5 d after germination growing on agar medium.

(B) Fluorescence image (left) and light image (right) of the *PIP5K3-YFP* root surface with an emerging bulge (arrow) and the position where a bulge was expected to emerge (arrowhead). Time-lapse fluorescence images of the same sample are shown in Supplemental Figure 5 online.

(C) An emerging bulge on the *PIP5K3-YFP* root hair cell surface.

(D) to **(G)** Elongating *PIP5K3-YFP* root hairs. The fluorescence intensity is shown by index colors, with red and blue for high and low intensities, respectively, in **(F)**.

(H) An elongating *PIP5K3ΔM-YFP* root hair.

Bars = 0.2 mm in **(A)**, 20 μ m in **(B)** to **(D)**, **(G)**, and **(H)**, and 10 μ m in **(E)** and **(F)**.

fluorescence localized most intensively to the apical plasma membrane (Figure 6).

Basically, the same pattern was observed for root hair bulges after they became apparent (Figures 5B and 5C; see Supplemental Figure 5 online). In an earlier stage, when a bulge was not recognizable, a weak fluorescence signal was detected at the position where a bulge was expected to appear (Figure 5B; see Supplemental Figure 5 online). On termination of root hair elongation, the apex-localized signal decreased, along with a reduction in the elongation rate, and almost disappeared before elongation stopped (Figure 7), consistent with the observation that mature root hairs did not exhibit YFP fluorescence (Figure 5A). By contrast, when a truncated fusion protein without the N-terminal MORN motif domain (PIP5K3 Δ M-YFP) was expressed by the *PIP5K3* promoter in *pip5k3* mutant plants, the short-root-

hair phenotype was not complemented (data not shown) and the YFP fluorescence was localized throughout the cytoplasm of root hairs (Figure 5H).

Inducible Overexpression of PIP5K3 Enhanced Root Hair Elongation and Increased the Rate of PtdIns(4,5)P₂ Production

To further analyze the biological function of PIP5K3 in planta, the gene was ectopically overexpressed by introducing an inducible gene expression system (Zuo et al., 2000) into the wild-type genetic background. The transgenic plants showed no phenotypic changes in the absence of the inducer, β -estradiol (Figure 8B), but when plants were transferred to an agar medium containing the inducer, they overexpressed the *PIP5K3* transgene (Figure 8A) and, more importantly, exhibited much longer root hairs than did noninduced plants or control plants that inducibly overexpressed GFP (Figures 8B to 8D). An abnormality was also found in the morphology of root hair cells. Multiple protruding sites or hair structures on the surface of a single trichoblast were often found, which were absent from wild-type roots (Figure 8E). In addition to straight long root hairs, winding root hairs were also observed in some lines (Figures 8F and 8G).

To obtain in planta evidence for the enzymatic activity of PIP5K3, the incorporation of ³²P-labeled phosphate into the phospholipids was measured in seedlings incubated overnight with and without the inducer. The amount of [³²P]PtdIns(4,5)P₂ was specifically increased in PIP5K3-overexpressing seedlings compared with those inducibly overexpressing GFP (Figure 9). These results show that PIP5K3 contributes to the production of PtdIns(4,5)P₂ also in planta and that PIP5K3 activity is a rate-limiting step for PtdIns(4,5)P₂ accumulation.

DISCUSSION

Of the 11 PIP5Ks in *Arabidopsis*, only the in vitro enzyme activity of PIP5K1, PIP5K4, and PIP5K10 have been characterized, preferentially catalyzing PtdIns(4,5)P₂ formation from PtdIns4P (Mikami et al., 1998; Elge et al., 2001; Westergren et al., 2001; Perera et al., 2005; Lee et al., 2007). The GST-PIP5K3 fusion protein also showed the 5-kinase activity in vitro, with a substrate preference for PtdIns4P. Consistently, seedlings inducibly overexpressing PIP5K3 had a significantly higher rate of PtdIns(4,5)P₂ production than control plants. The in vitro and in vivo evidence, together with the expression pattern of the *PIP5K3* gene, indicate that PIP5K3 acts as a PtdIns4P 5-kinase in *Arabidopsis* root hair cells. Furthermore, the *PIP5K3* promoter-driven PIP5K3-YFP could complement the *pip5k3* mutant defect, and the localization of the fluorescence signal coincided with that of PtdIns(4,5)P₂ (Vincent et al., 2005; van Leeuwen et al., 2007). From these results, we conclude that PIP5K3 is involved in establishing the spatiotemporal pattern of PtdIns(4,5)P₂ during root hair development.

Based on the low levels (*pip5k3-1* and *pip5k3-3*) or abnormalities (*pip5k3-2* and *pip5k3-4*) of the mutant transcripts, it is thought that the short-root-hair phenotype was caused by a shortage of functional PIP5K3 protein in all cases. This idea

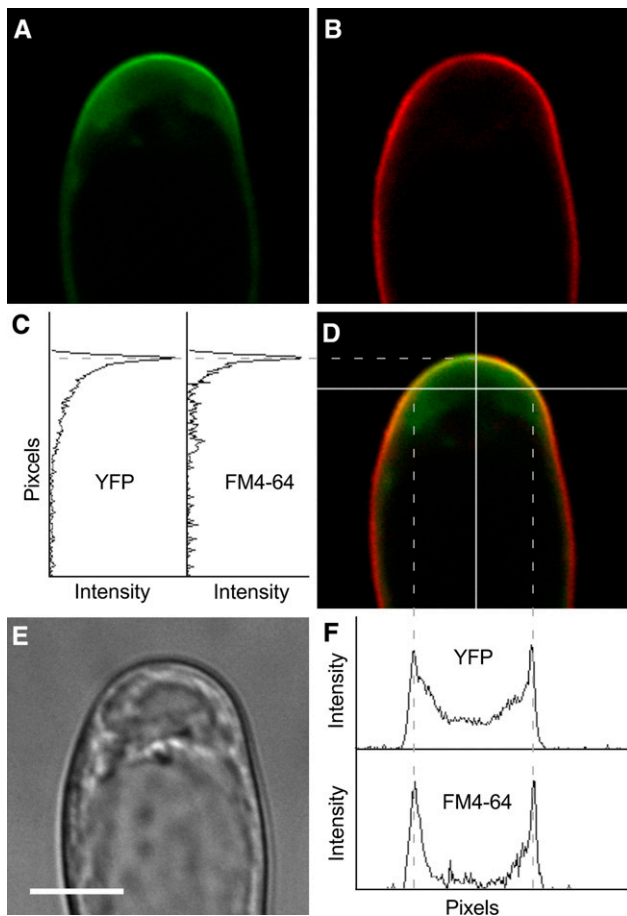


Figure 6. Colocalization of Fluorescence Signals in a *PIP5K3*-YFP Root Hair Stained with FM4-64.

The YFP (A) and FM4-64 (B) fluorescence signals were observed in an elongating *PIP5K3*-YFP root hair by confocal laser scanning microscopy. The overlay fluorescence image (D) and a bright-field image (E) are also shown. The intensity of each fluorescence signal was scanned along the white lines on the overlay image. The results of vertical (C) and horizontal (F) scans are shown graphically. Dashed lines indicate the positions at which peaks of both fluorescence signals were colocalized. Bar = 10 μ m.

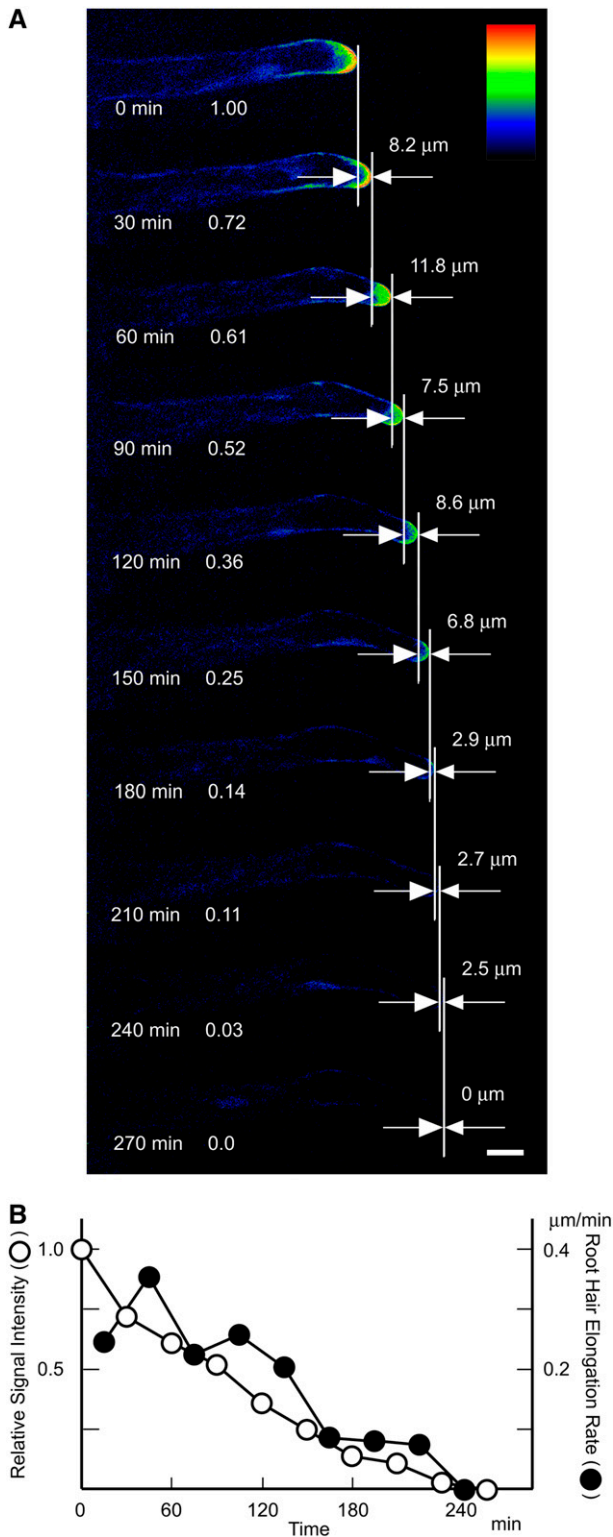


Figure 7. Continuous Observation of a *PIP5K3*-YFP Root Hair Ceasing Elongation.

(A) The YFP fluorescence of an elongating *PIP5K3*-YFP root hair was observed every 30 min by confocal laser scanning microscopy until root

is supported by the observation that the phenotype of all four mutant alleles could be complemented with the *PIP5K3* promoter-driven *PIP5K3* or *PIP5K3*-YFP transgene (see Supplemental Figure 6 online). The severity of the phenotype suggests that *PIP5K3* contributes substantially to the production of $\text{PtdIns}(4,5)\text{P}_2$ required for root hair elongation. Although these mutant lines had short root hairs, their morphology appeared to be normal. This is in contrast with the short and distorted root hairs seen in the *cow1/sfh1* mutants and the *pi-4kβ1 pi-4kβ2* double mutant, both of which contain defects in the phosphoinositide metabolic pathway leading to $\text{PtdIns}(4,5)\text{P}_2$ production (Bohme et al., 2004; Vincent et al., 2005; Preuss et al., 2006). There may be several reasons for this. First, since none of the four *pip5k3* mutants were determined to be null alleles, residual levels of *PIP5K3* activity in the mutant root hair cells may satisfy the minimum requirements of root hair morphogenesis. Alternatively, other *PIP5Ks* may provide the minimum level of $\text{PtdIns}(4,5)\text{P}_2$ in root hairs. Although $\text{PtdIns}(4,5)\text{P}_2$ levels in mutant root hair cells are unknown, based on the essential function of $\text{PtdIns}(4,5)\text{P}_2$ in animal and fungal cell morphogenesis, it is reasonable to assume that significant amounts of $\text{PtdIns}(4,5)\text{P}_2$ remain present. Second, it is also possible that PtdIns , $\text{PtdIns}4\text{P}$, and their metabolites other than $\text{PtdIns}(4,5)\text{P}_2$ play essential signaling roles in root hair morphogenesis and, hence, that a defect in *PIP5K3* alone had a more limited effect than defects in enzymes acting upstream in the phosphoinositide metabolic pathway. Supporting this idea, the *pi-4kβ1 pi-4kβ2* double mutation is assumed to cause an abnormality in the *trans*-Golgi network through a shortage of $\text{PtdIns}4\text{P}$ (Preuss et al., 2006).

In the expression analysis using the *GUS* reporter gene directed by the *PIP5K3* promoter, *GUS* activity was detected in root hair cell files, relatively more strongly in the part containing developing root hair cells compared with the more basal part containing mature root hair cells. In the RT-PCR analysis of the basal and apical parts of the roots, a much larger difference between the basal and apical parts was detected than in the *GUS* reporter analysis. Assuming that the result of the RT-PCR analysis reflects actual steady state levels of the *PIP5K3* transcript, the *GUS* transcript or protein might be more stable than the *PIP5K3* transcript in root hair cells. Furthermore, when the same *PIP5K3* promoter directed the *PIP5K3*-YFP protein, the YFP fluorescence was detected only in developing root hair cells and not in mature root hair cells. Translational or posttranslational regulation may limit the *PIP5K3* protein to developing root hair cells. For the other *PIP5K* genes, such a specific expression pattern has not been observed (Mikami et al., 1998; Perera et al., 2005; Lee et al., 2007; Lou et al., 2007), suggesting that the *PIP5K3* gene has evolved to have a specific function in root hair development. To date, the biological functions of *PIP5K1* and

hair elongation ceased. This is shown as index colors, with red and blue for high and low intensities, respectively. The elapsed time and the relative intensity of the fluorescence signal detected in a 15- μm region in the apex are indicated at left in each image. The increase in root hair length at 30 min is indicated at right in each image. Bar = 20 μm .

(B) The relative signal intensity and the root hair elongation rate are shown graphically with the elapsed time.

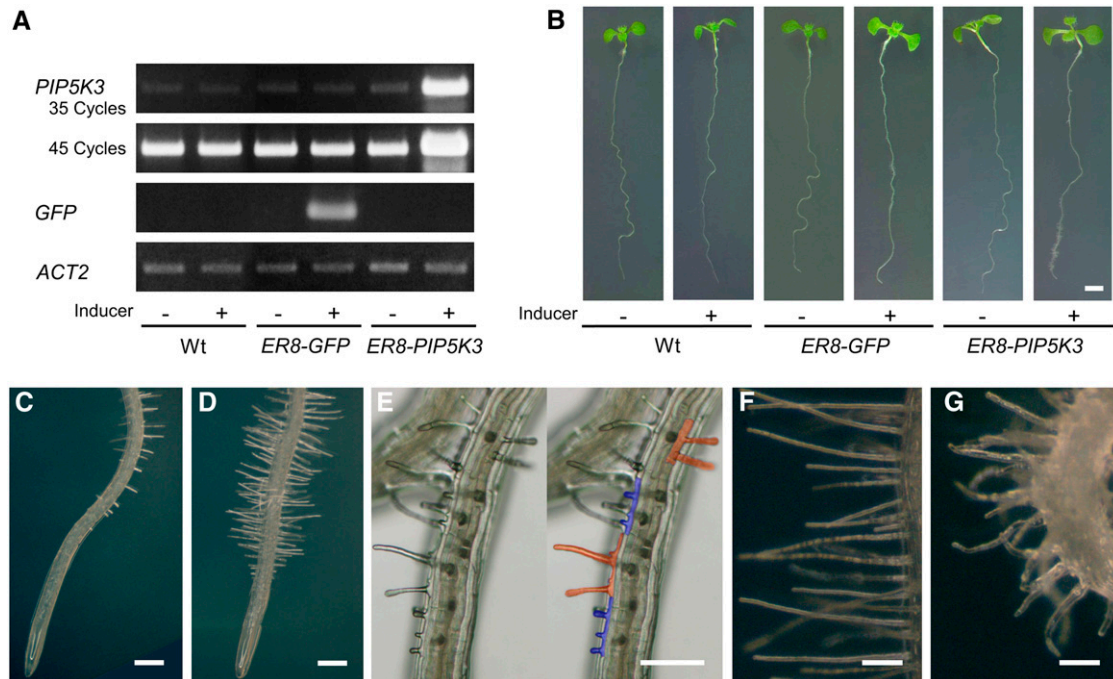


Figure 8. Phenotypes Caused by Inducible Overexpression of *PIP5K3* in Roots.

(A) RT-PCR analysis of inducible gene expression. Total RNA was prepared from uninduced (–) and induced (+) wild-type, *ER8-GFP*, and *ER8-PIP5K3* seedlings. *PIP5K3* cDNA was amplified for 35 and 45 PCR cycles, *GFP* cDNA was amplified for 25 cycles, and *ACT2* cDNA was amplified for 20 cycles. Products were electrophoresed on agarose gels and stained with ethidium bromide. Three biological replicates showed the same result.

(B) Phenotypic changes in seedlings caused by inducible gene expression. Uninduced (–) and induced (+) wild-type, *ER8-GFP*, and *ER8-PIP5K3* seedlings are shown.

(C) and **(D)** Root phenotypes. Uninduced **(C)** and induced **(D)** roots of the same *ER8-PIP5K3* line are shown.

(E) to **(G)** Root surface of the induced *ER8-PIP5K3* line. Cells with multiple protruding sites are highlighted with colors at right in **(E)** so that individual cells can be clearly identified. Straight long root hairs and winding root hairs observed in different *ER8-PIP5K3* lines are shown in **(F)** and **(G)**, respectively.

Bars = 2 mm in **(B)**, 0.2 mm in **(C)** to **(E)**, and 0.1 mm in **(F)** and **(G)**.

PIP5K9 have been assumed to be signal transduction for overall cell responses to abscisic acid and sugar, respectively (Mikami et al., 1998; Elge et al., 2001; Lou et al., 2007). By contrast, PIP5K3 seems to act as a signaling protein for an intracellular site-specific event. In plants expressing PIP5K3-YFP, the fluorescence signal localized to growing root hairs and seemed to anticipate root hair growth. The signal disappeared from the apices before root hair elongation was complete. This spatio-temporal pattern indicates that PIP5K3 is one of the factors leading to cell expansion rather than a result of cell expansion.

Using transgenic tobacco (*Nicotiana tabacum*) cells expressing a mammalian PIP5K, it was recently shown that PIP5K is the flux-limiting factor in the plant metabolic pathway that leads to PtdIns(4,5)P₂ production (Im et al., 2007b). In our study, reduced *PIP5K3* expression levels in the mutant lines or increased levels following inducible overexpression caused significantly shorter or longer root hairs, respectively, than normal. Moreover, transgenic plants with higher expression levels of PIP5K3-YFP tended to have longer root hairs. These results strongly suggest that the expression level of *PIP5K3* is a rate-limiting factor in root hair elongation. Together, these observations suggest that the ac-

cumulation of PtdIns(4,5)P₂ in the root hair apex is a key factor promoting root hair elongation. In pollen tube tip growth, phospholipase C (PLC), an enzyme that degrades PtdIns(4,5)P₂, localizes laterally at the tip plasma membrane and restricts a PtdIns(4,5)P₂-rich region to the apex (Dowd et al., 2006; Helling et al., 2006). PIP5K and PLC might regulate the amount and distribution of PtdIns(4,5)P₂ at the tip-growing apex, respectively. Although PLC activity has not been identified in root hair cells, PLC might be another major player that regulates PtdIns(4,5)P₂ localization in root hair development.

Overexpression of *PIP5K3* often resulted in multiple protruding structures on the surface of a single trichoblast. This phenotype is similar to that caused by mutations in *SCN1* and the overexpression of *ROP2* (Jones et al., 2002; Carol et al., 2005). Moreover, in the *PIP5K3-YFP* plants, the localization of the fluorescence signal to the site of future bulge formation is similar to that of ROPs (Molendijk et al., 2001; Jones et al., 2002). This strongly suggests that PIP5K3, together with ROPs, is involved in establishing the planar polarity of bulge initiation. During root hair growth, the signal localization to elongating root hair apices is also similar to that of ROPs, and in both PIP5K3- and

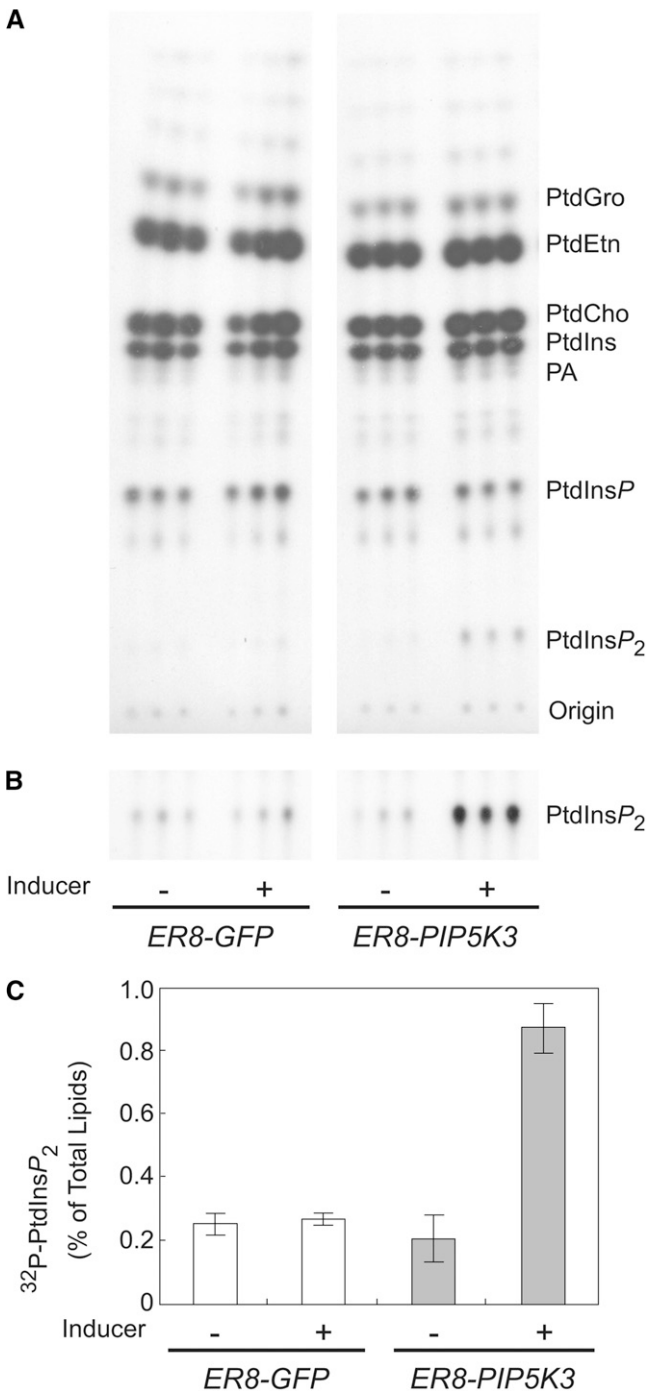


Figure 9. Increased PtdIns(4,5)P₂ Levels of Seedlings Overexpressing PIP5K3.

Lipids were extracted from uninduced (–) and induced (+) *ER8-GFP* and *ER8-PIP5K3* seedlings, analyzed by thin layer chromatography, and quantified by phosphoimaging. Each sample is represented by three seedlings, with analysis performed in triplicate.

(A) Thin layer chromatography image of ³²P-labeled phospholipids. Results from a representative experiment are shown ($n = 3$). The positions of phospholipids and the origin are marked. PtdCho, phosphatidylcholine; PtdEtn, phosphatidylethanolamine; PtdGro, phosphatidylglycerol.

ROP2-overexpressing plants, long and winding root hairs can be observed (Molendijk et al., 2001; Jones et al., 2002). These data suggest that PIP5K3 may function as a downstream effector of ROPs in regulatory mechanisms, not only for the planar polarity of bulge initiation but also for the promotion of root hair tip growth. Prolonged overexpression of *PIP5K3* suppressed root growth, which did not occur when GFP was overexpressed (see Supplemental Figure 7 online). A similar phenotype has also been observed in plants ectopically overexpressing PIP5K9, although no increase in root hair length was reported (Lou et al., 2007). The effect of overexpression on root growth, but not on root hair development, might be common to PIP5Ks from the B subfamily.

In elongating root hair apices of the *PIP5K3-YFP* plants, the fluorescence signal intensively localized to the plasma membrane. However, a considerable amount of the signal could also be observed in the cytoplasmic space of root hair apices, whereas it was not detected in other cytoplasmic spaces, including those surrounding nuclei. By contrast, the truncated fusion protein without the MORN motif domain diffused to all cytoplasmic spaces. The cytoplasmic space of elongating root hair apices is referred to as the vesicle-rich zone and contains high concentrations of small vesicles and a fine configuration of F-actin (Braun et al., 1999). Hence, it is reasonable to suggest that PIP5K3 does not diffuse into the cytoplasm but is anchored directly or indirectly to structures in the vesicle-rich zone. Given that PtdIns(4,5)P₂ and PA activate PIP5K1 through binding to the MORN motif domain in vitro (Im et al., 2007a), PIP5K3 might be recruited and activated by these phospholipids through the MORN motif domain. Since PA can be generated by PLDζ1, which is a positive regulator of root hair development (Ohashi et al., 2003), and activated by PtdIns(4,5)P₂ in vitro (Qin and Wang, 2002), a positive feedback loop between PIP5K3 and PLDζ1 may be generated to amplify the signal, similar to what has been proposed for animal cells (Oude Weernink et al., 2007). In animal systems, in which the PtdInsP kinases lack the MORN motif, small GTPases such as Rho and Arf have been proposed as key regulators (Santarius et al., 2006). The apparent colocalization of ROP and PIP5K3 during root hair development might reflect the recruitment and/or regulation of PIP5K3 by ROPs. In tobacco pollen tubes, *Arabidopsis* ROP7/Rac2 has been reported to localize to the apical plasma membrane and to physically interact with PIP5K activity (Kost et al., 1999), supporting this suggestion. Although direct interactions between PIP5K3 and these candidates remain to be examined, it is likely that many interactions among signaling proteins and phospholipids are involved in the localization, as proposed in animal systems (Di Paolo and De Camilli, 2006).

In this study, we demonstrated the involvement of *PIP5K3* in root hair development by genetic analysis. The analyses of enzyme activity, gene expression, and intracellular localization revealed that PIP5K3 is involved in localizing PtdIns(4,5)P₂ to the elongating root hair apex. From these observations, together with

(B) Longer exposure thin layer chromatography image of ³²P-labeled PtdIns(4,5)P₂.

(C) Quantification of ³²P-labeled PtdIns(4,5)P₂. The means and SD are indicated by the white and gray bars and error bars ($n = 3$), respectively.

the striking overlaps in the presumed spatiotemporal localization patterns and overexpression phenotypes of PIP5K3 and ROPs, we conclude that PIP5K3 is part of the mechanism that positively regulates root hair initiation and growth. For further understanding of the mechanism regulating root hair tip growth, interactions between PIP5K3 and other signaling factors that are assumed to be involved in cell morphogenesis should be investigated.

METHODS

Plant Material and Growth Conditions

All *Arabidopsis thaliana* lines used were in the Columbia background, and Columbia was used as the wild type. The T-DNA insertion lines SALK_001546, SALK_060590, SALK_000024, and SALK_026683 were identified in the collection of the Salk Institute Genomic Analysis Laboratory (Alonso et al., 2003) and obtained from the ABRC. *Arabidopsis* plants were grown on Murashige and Skoog medium containing 0.8% agar, B5 vitamins, and 1% sucrose, under 16 h of light and 8 h of dark at 22°C, or on soil under continuous light at 22°C, unless noted otherwise. Inducible overexpression was performed by transferring seedlings grown on vertical standing 2% agar medium for 4 d after germination onto standing agar medium with 10 μ M β -estradiol and then growing them for 1 d for RT-PCR analysis or for 3 d for the observation of phenotypic changes.

Transgene Constructs and *Arabidopsis* Transformation

A 1.2-kb DNA fragment encompassing the region between the termination codon of the upstream neighboring gene and the *PIP5K3* initiation codon was amplified by PCR using *Arabidopsis* genomic DNA as a template. To construct the *PIP5K3* promoter-GUS gene, the PCR fragment was substituted for the 35S promoter region in the binary vector pBI121 using the *Hind*III and *Bam*HI sites of the vector. The junctions upstream and downstream of the PCR fragment were 5'-AAGCTTATC-TTCTTGTCATCTACAT-3' and 5'-ATAATAATGCAAGACAGGATCC-3', respectively (the underlined sequences are the restriction sites of pBI121). A cDNA fragment encoding full-length PIP5K3 was synthesized and amplified from an *Arabidopsis* poly(A) RNA fraction, using the SuperScript One-Step RT-PCR kit containing Platinum *Taq* (Invitrogen) and the primers 5'-CCCCCCGGGATGCAAGACAGTGTCC-3' and 5'-CCCCTCTAGAGAACTTGTGTAGGTGTGCAC-3' (the underlined sequences are the overhangs containing restriction sites for cloning), and cloned into pUC19 using the *Sma*I and *Xba*I sites. To construct the *PIP5K3-YFP* gene, a DNA fragment encoding EYFP (BD Biosciences Clontech) was fused to the PIP5K3 coding fragment in an in-frame manner. The junction sequence between the two coding sequences was 5'-GACAAATGGGTACCGTCCGCCACCATG-3' (the sequences encoding the C-terminal amino acids of PIP5K3 and the initiation codon of EYFP are underlined). For the *PIP5K3 Δ M-YFP* gene, the region corresponding to the amino acids from position 5 to 300 of PIP5K3 was deleted in an in-frame manner. To construct the *PIP5K3* promoter-driven *PIP5K3*, *PIP5K3-YFP*, and *PIP5K3 Δ M-YFP* genes, the sequences encoding the proteins preceded by the promoter fragment were substituted for the promoter-GUS region of a pBI121-derived binary vector, pHPT121, in which the kanamycin resistance gene in the T-DNA of pBI121 was replaced with a hygromycin resistance gene. The sequences of the junctions upstream of the coding sequences were 5'-CATATATAA-TAATGCAAGACAGTG-3' for *PIP5K3* and *PIP5K3-YFP* and 5'-CATA-TATAATAATGCAAGACAGGATCCATGAGTGT-3' for *PIP5K3 Δ M-YFP* (the initiation codons are underlined). The sequences of the junctions downstream of the coding sequences were 5'-TGAATTCTAGTCC-

GAGCTC-3' for *PIP5K3* and 5'-TAAAGCGCCGCGACTCTAGA-3' for *PIP5K3-YFP* and *PIP5K3 Δ M-YFP* (the termination codons are underlined). To construct the inducible *PIP5K3* gene, a PIP5K3-coding fragment was inserted between the *Xho*I and *Spe*I sites of pER-8 (Zuo et al., 2000). The junction sequences were 5'-CTCGAGGGATG-3' and 5'-TGAATTAAGTAACGTGCAACACCTACACAAGTTCTCTAGT-3', respectively (the initiation and termination codons of PIP5K3 are underlined). Strains of *Agrobacterium tumefaciens* LBA4404 carrying each construct were used to transform *Arabidopsis* by vacuum infiltration. The resulting transgenic plants were self-pollinated, and T3 plants homozygous for the transgene were used in subsequent experiments.

RNA Gel Blot Analysis

For organ-specific expression analysis of PIP5K genes, total RNA fractions were prepared from seedpods and pollinated flowers, rosette leaves, stems, and inflorescences without pollinated flowers of plants grown on soil as well as from roots of plants grown for 21 d on vertically standing 2% agar medium. RNA gel blot hybridizations were performed according to the instructions for the Hybond-N blotting membrane (GE Healthcare). The regions of cDNA used as probes were 1859 to 2259 for PIP5K1, 1865 to 2265 for PIP5K2, 1 to 653 for PIP5K3, 491 to 839 for PIP5K4, 471 to 917 for PIP5K5, 1 to 535 for PIP5K6, 316 to 737 for PIP5K7, 201 to 642 for PIP5K8, 422 to 1308 for PIP5K9, 450 to 1251 for PIP5K10, and 528 to 1139 for PIP5K11 (numbers correspond to nucleotide positions starting at the 5' ends of the coding regions).

RT-PCR Analysis

Total RNA was isolated from roots of 5-d-old plants using RNeasy (Qiagen) unless noted otherwise. Roots of plants grown on vertical standing 2% agar medium for 5 d after germination were separated into apical and basal parts by cutting them 5 mm from the root apex. RT-PCR analysis was performed using total RNA prepared from the apical and basal parts of roots. RT-PCR analysis for the detection of *PIP5K3* transcripts was performed using total RNA prepared from roots of the wild-type and mutant lines grown on vertical standing 2% agar medium for 5 d after germination. To detect transcripts of the *PIP5K3* gene and the *PIP5K3* transgene, first-strand cDNA was synthesized and amplified with the SuperScript One-Step RT-PCR kit containing Platinum *Taq* using total RNA and the *PIP5K3*-specific primers 5'-AGGTAATCTGTTGGGAAACATGCTTCC-3' and 5'-CAAATCTGCTCACCTGCTCTGCTT-3'. As a control, primers specific to the *ACT2* gene (gene locus, At3g18780), 5'-TGG-TGTCATGGTTGGGATG-3' and 5'-CACCACCTGAGCACAATGTTAC-3', and the GFP gene (Niwa et al., 1999), 5'-CAAGCTGACCCTGAAGTTCATCTG-3' and 5'-ACGAACTCCAGCAGGACCATGTGAT-3', were used. To determine the 5' structure of *pip5k3-2* mutant transcripts, upstream primers in the 5' untranslated region, 5'-GATTTTGATTATTC-TAATTTTCATTGATCAG-3', 5'-TTTCATTCAGATTTAGCATCAAAGT-3', 5'-TTA-GGGTCATTATTGATCACCTTTGT-3', and 5'-GAACACTAAATGTTATTG-GAAGAGAC-3', an upstream primer in the T-DNA region, 5'-CCT-GTTGCCGCTCTTGGCGATGATT-3', and a downstream primer, 5'-GGA-CTTTGTTGAACACTCATGGCAC-3', were used. To determine the 3' structure of *pip5k3-4* mutant transcripts, an upstream primer, 5'-CTTGACTCAAGAT-GAACGCTAC-3', and a downstream primer in the T-DNA region, 5'-GCG-GTGTCTATCTATGTTACTAGATCG-3', were used. PCR products were fractionated by agarose gel electrophoresis and stained with ethidium bromide.

In Vitro Phosphoinositide Kinase Assay

To construct the recombinant protein, GST-PIP5K3, a DNA fragment encoding PIP5K3, was cloned into the expression vector pGEX-6P1 (GE Healthcare) in-frame with the GST-coding sequence. The junction

sequence between the GST- and PIP5K3-coding regions was 5'-GGG-GCCCTGGGATCCATGCAAGAG-3' (the initiation codon of PIP5K3 is underlined). To express the recombinant protein, an overnight culture of *Escherichia coli* BL21(DE3)-CodonPlus (Stratagene) carrying the constructed plasmid was diluted 10-fold into L-broth and incubated with shaking at 37°C for 1 h. The culture was then transferred to 18°C, and isopropyl- β -D-thiogalactoside was added to a final concentration of 0.5 mM. Incubation was continued for 6 h, and cells were collected by centrifugation. The cells were suspended in PBS buffer (1.8 mM KH₂PO₄, 10.1 mM Na₂HPO₄, 140 mM NaCl, and 2.7 mM KCl, pH 7.3), sonicated on ice, and centrifuged at 12,000g for 15 min at 4°C. The supernatant was mixed with glutathione-Sepharose 4B (GE Healthcare) and incubated at 4°C for 2 h with gentle shaking. The Sepharose beads were collected and washed with an excess volume of PBS.

Lipid kinase activity was assayed on purified GST-PIP5K3 or GST protein attached to the glutathione beads (10 μ L). As positive control proteins, 1 μ g each of Myc-tagged mammalian type I and II PtdInsP kinases, purified from *E. coli* and COS cells, respectively, was used (Meijer et al., 2001). Synthetic PtdInsPs were obtained from Echelon; all other lipids were from Avanti Polar Lipids. Kinase assays and lipid extractions were performed as described previously (Meijer et al., 2001). Lipid mixtures, consisting of 10 nmol of phosphatidylserine, 3 nmol of PA, and 1 nmol of PtdIns4P or PtdIns5P, were prepared in chloroform, dried down, rehydrated, and sonicated in 10 mM Tris, pH 7.5. Reactions were performed in a volume of 40 μ L for 90 min in the presence of 55 mM Tris, pH 7.5, 10 mM MgCl₂, 1 mM EGTA, 70 mM KCl, 25 μ M ATP, and 5 μ Ci of [γ -³²P]ATP. Reactions were stopped by adding 1 mL of chloroform:methanol (1:1) and 300 μ L of 2 M HCl. Lipids were extracted, separated by alkaline thin layer chromatography, and visualized by phosphoimaging (Meijer et al., 2001).

PtdInsP₂ Measurements in Planta

Arabidopsis seedlings grown for 5 d after germination were labeled overnight in 400 μ L of 2.5 mM MES, 1 mM KCl, pH 5.7, containing 5 μ Ci of carrier-free ³²Pi (Amersham PBS 11), and either 10 μ M β -estradiol or 0.1% DMSO (control). For each sample, three seedlings were taken and experiments were routinely executed in triplicate. After 16 h, labeling was stopped by adding perchloric acid to a final concentration of 5% (v/v) and extracting the lipids into chloroform:methanol as described earlier (Meijer et al., 1999; Den Hartog et al., 2001). Accordingly, lipids were analyzed by thin layer chromatography and quantified by phosphoimaging.

GUS Staining

Histochemical GUS analysis was performed as described previously (Imajuku et al., 2001) on seedlings containing the reporter gene grown for 4 d after germination on agar medium.

Microscopy

The fluorescence of YFP and FM4-64 (Anaspec) was observed with a CSU22 confocal scanner unit (Yokogawa) and a CCD camera (ORCA ER C4742-80; Hamamatsu Photonics) on an Axiovert 200M apparatus (Carl Zeiss). Root hairs were treated with 1.6 μ M FM4-64 prior to imaging. Both signals were observed simultaneously within 3 min after the FM4-64 treatment. Excitation beams of 488 and 568 nm, and detection bands of 520 to 555 nm and 580 to 630 nm, were used for YFP and FM4-64, respectively. IPLab version 3.71 (BD Biosciences Bioimaging) was used for image processing.

Accession Numbers

Sequence data from this article can be found in the GenBank/EMBL data libraries under accession numbers AB005902 (*PIP5K1*), NM_106423

(*PIP5K2*), MN_128199 (*PIP5K3*), NM_115555 (*PIP5K4*), NM_129686 (*PIP5K5*), MN_111675 (*PIP5K6*), NM_100965 (*PIP5K7*), NM_104770 (*PIP5K8*), NM_111827 (*PIP5K9*), NM_100028 (*PIP5K10*), NM_116349 (*PIP5K11*), and NM_112764 (*ACT2*).

Supplemental Data

The following materials are available in the online version of this article.

Supplemental Figure 1. RNA Gel Blot Analysis of *Arabidopsis* PIP5K Genes.

Supplemental Figure 2. Sequence Information of Mutant Transcripts.

Supplemental Figure 3. Distributions of Root Hair Lengths of Wild-Type, Mutant, and Complementation Lines.

Supplemental Figure 4. Apices of Wild-Type and Mutant Root Hairs.

Supplemental Figure 5. Continuous Observation of PIP5K3-YFP in the Sites of Bulge Formation.

Supplemental Figure 6. Complementation of the Mutant Phenotype by the *PIP5K3* and *PIP5K3-YFP* Transgenes.

Supplemental Figure 7. Phenotype Caused by Prolonged Overexpression of *PIP5K3*.

Supplemental Movie 1. Time-Lapse Observation of PIP5K3-YFP in an Elongating Root Hair.

ACKNOWLEDGMENTS

We thank K. Yasuda and G. Gonorazky for technical assistance, N.-H. Chua for providing the estrogen-inducible gene expression system, N. Divecha for providing the mammalian type I and type II PtdInsP kinases, and Y. Niwa for providing the GFP coding fragment. This work was supported by awards from the Japanese Society for the Promotion of Science (JSPS), the Kyoto University Alliance for Chemistry of the 21st Century COE Program, and the Institute for Chemical Research of Kyoto University to H.K.; by Netherlands Organization for Scientific Research (NWO) Grant CW VIDI 700.56.429 to C.T.; by grants from the NWO (Grants ALW 863.04.004 and VIDI 864.05.001), the European Commission (Grant HPRN-CT-2002-00251), and the Royal Netherlands Academy of Arts and Sciences to T.M.; and by grants from the JSPS (Grant-in-Aid for Scientific Research-B 16370023) and the Ministry of Education, Culture, Sports, Science, and Technology, Japan (Grant-in-Aid for Scientific Research on Priority Areas 18056012) to T.A.

Received October 7, 2007; revised January 4, 2008; accepted January 30, 2008; published February 15, 2008.

REFERENCES

- Alonso, J.M., et al. (2003). Genome-wide insertional mutagenesis of *Arabidopsis thaliana*. *Science* **301**: 653–657.
- Anthony, R.G., Henriques, R., Helfer, A., Meszaros, T., Rios, G., Testerink, C., Munnik, T., Deak, M., Koncz, C., and Bogre, L. (2004). A protein kinase target of a PDK1 signalling pathway is involved in root hair growth in *Arabidopsis*. *EMBO J.* **23**: 572–581.
- Aoyagi, K., Sugaya, T., Umeda, M., Yamamoto, S., Terakawa, S., and Takahashi, M. (2005). The activation of exocytotic sites by the formation of phosphatidylinositol 4,5-bisphosphate microdomains at syntaxin clusters. *J. Biol. Chem.* **280**: 17346–17352.
- Bohme, K., Li, Y., Charlot, F., Grierson, C., Marrocco, K., Okada, K.,

- Laloue, M., and Nogue, F.** (2004). The *Arabidopsis* *COW1* gene encodes a phosphatidylinositol transfer protein essential for root hair tip growth. *Plant J.* **40**: 686–698.
- Braun, M., Baluska, F., von Witsch, M., and Menzel, D.** (1999). Redistribution of actin, profiling and phosphatidylinositol-4,5-bisphosphate in growing and maturing root hairs. *Planta* **209**: 435–443.
- Carol, R.J., and Dolan, L.** (2006). The role of reactive oxygen species in cell growth: Lessons from root hairs. *J. Exp. Bot.* **57**: 1829–1834.
- Carol, R.J., Takeda, S., Linstead, P., Durrant, M.C., Kakesova, H., Derbyshire, P., Drea, S., Zarsky, V., and Dolan, L.** (2005). A RhoGDP dissociation inhibitor spatially regulates growth in root hair cells. *Nature* **438**: 1013–1016.
- Cole, R.A., and Fowler, J.E.** (2006). Polarized growth: Maintaining focus on the tip. *Curr. Opin. Plant Biol.* **9**: 579–588.
- Den Hartog, M., Musgrave, A., and Munnik, T.** (2001). Nod factor-induced phosphatidic acid and diacylglycerol pyrophosphate formation: A role for phospholipase C and D in root hair deformation. *Plant J.* **25**: 55–65.
- Di Paolo, G., and De Camilli, P.** (2006). Phosphoinositides in cell regulation and membrane dynamics. *Nature* **443**: 651–657.
- Dolan, L., Janmaat, K., Willemsen, V., Linstead, P., Poethig, S., Roberts, K., and Scheres, B.** (1993). Cellular organization of the *Arabidopsis thaliana* root. *Development* **119**: 71–84.
- Dowd, P.E., Coursol, S., Skirpan, A.L., Kao, T., and Gilroy, S.** (2006). *Petunia* phospholipase C1 is involved in pollen tube growth. *Plant Cell* **18**: 1438–1453.
- Downes, C.P., Gray, A., and Lucocq, J.M.** (2005). Probing phosphoinositide functions in signaling and membrane trafficking. *Trends Cell Biol.* **15**: 259–268.
- Elge, S., Brearley, C., Xia, H.-J., Kehr, J., Xue, H.-W., and Mueller-Roeber, B.** (2001). An *Arabidopsis* inositol phospholipid kinase strongly expressed in procambial cells: Synthesis of PtdIns(4,5)P₂ and PtdIns(3,4,5)P₃ in insect cells by 5-phosphorylation of precursors. *Plant J.* **26**: 561–571.
- Fischer, U., Shuzhen, M., and Grebe, M.** (2004). Lipid function in plant cell polarity. *Curr. Opin. Plant Biol.* **7**: 670–676.
- Foreman, J., Demidchik, V., Bothwell, J.H.F., Mylona, P., Miedema, H., Torres, M.A., Linstead, P., Costa, S., Brownlee, C., Jones, J.D.G., Davies, J.M., and Dolan, L.** (2003). Reactive oxygen species produced by NADPH oxidase regulate plant cell growth. *Nature* **422**: 442–446.
- Gilroy, S., and Jones, D.L.** (2000). Through form to function: Root hair development and nutrient uptake. *Trends Plant Sci.* **5**: 56–60.
- Grishanin, R.N., Kowalchuk, J.A., Klenchin, V.A., Ann, K., Earles, C.A., Chapman, E.R., Gerona, R.R.L., and Martin, T.F.J.** (2004). CAPS acts at a prefusion step in dense-core vesicle exocytosis as a PIP₂ binding protein. *Neuron* **43**: 551–562.
- Helling, D., Possart, A., Cottier, S., Klahre, U., and Kost, B.** (2006). Pollen tube tip growth depends on plasma membrane polarization mediated by tobacco PLC3 activity and endocytic membrane recycling. *Plant Cell* **18**: 3519–3534.
- Hepler, P.K., Vidali, L., and Cheung, A.Y.** (2001). Polarized cell growth in higher plants. *Annu. Rev. Cell Dev. Biol.* **17**: 159–187.
- Im, Y.J., Davis, A.J., Perera, I.Y., Johannes, E., Allen, N.S., and Boss, W.F.** (2007a). The N-terminal membrane occupation and recognition nexus domain of *Arabidopsis* phosphatidylinositol phosphate kinase 1 regulates enzyme activity. *J. Biol. Chem.* **282**: 5443–5452.
- Im, Y.J., Perera, I.Y., Brglez, I., Davis, A.J., Stevenson-Paulik, J., Phillippy, B.Q., Johannes, E., Allen, N.S., and Boss, W.F.** (2007b). Increasing plasma membrane phosphatidylinositol(4,5)bisphosphate biosynthesis increases phosphoinositide metabolism in *Nicotiana tabacum*. *Plant Cell* **19**: 1603–1616.
- Imajuku, Y., Ohashi, Y., Aoyama, T., Goto, K., and Oka, A.** (2001). An upstream region of the *Arabidopsis thaliana* *CDKA;1* (*CDC2aAt*) gene directs transcription during trichome development. *Plant Mol. Biol.* **46**: 205–213.
- Jones, M.A., Raymond, M.J., and Smirnov, N.** (2006). Analysis of the root-hair morphogenesis transcriptome reveals the molecular identity of six genes with roles in root-hair development in *Arabidopsis*. *Plant J.* **45**: 83–100.
- Jones, M.A., Shen, J.-J., Fu, Y., Li, H., Yang, Z., and Grierson, C.S.** (2002). The *Arabidopsis* Rop2 GTPase is a positive regulator of both root hair initiation and tip growth. *Plant Cell* **14**: 763–776.
- Kost, B., Lemichez, E., Spielhofer, P., Hong, Y., Tolias, K., Carpenter, C., and Chua, N.-H.** (1999). Rac homologues and compartmentalized phosphatidylinositol 4,5-bisphosphate act in a common pathway to regulate polar pollen tube growth. *J. Cell Biol.* **145**: 317–330.
- Krauss, M., and Haucke, V.** (2007). Phosphoinositides: Regulators of membrane traffic and protein function. *FEBS Lett.* **581**: 2105–2111.
- Lee, Y., Kim, Y.-W., Jeon, B.W., Park, K.-Y., Suh, S.J., Seo, J., Kwak, J.M., Martinoia, E., Hwang, I., and Lee, Y.** (2007). Phosphatidylinositol 4,5-bisphosphate is important for stomatal opening. *Plant J.* **52**: 803–816.
- Li, L., Shin, O.-H., Rhee, J.-S., Arac, D., Rah, J.-C., Rizo, J., Sudhof, T., and Rosenmund, C.** (2006). Phosphatidylinositol phosphates as co-activators of Ca²⁺ binding to C₂ domains of synaptotagmin 1. *J. Biol. Chem.* **281**: 15845–15852.
- Logan, M.R., and Mandato, C.A.** (2006). Regulation of the actin cytoskeleton by PIP2 in cytokinesis. *Biol. Cell* **98**: 377–388.
- Lou, Y., Gou, J.-Y., and Xue, H.-W.** (2007). PIP5K9, an *Arabidopsis* phosphatidylinositol monophosphate kinase, interacts with a cytosolic invertase to negatively regulate sugar-mediated root growth. *Plant Cell* **19**: 163–181.
- Meijer, H.J.G., Berrie, C.P., Iurisci, C., Divecha, N., Musgrave, A., and Munnik, T.** (2001). Identification of a new polyphosphoinositide in plants, phosphatidylinositol 5-monophosphate (PtdIns5P), and its accumulation upon osmotic stress. *Biochem. J.* **360**: 491–498.
- Meijer, H.J.G., Divecha, N., van den Ende, H., Musgrave, A., and Munnik, T.** (1999). Hyperosmotic stress induces rapid synthesis of phosphatidyl-D-inositol 3,5-bisphosphate in plant cells. *Planta* **208**: 294–298.
- Meijer, H.J.G., and Munnik, T.** (2003). Phospholipid-based signaling in plants. *Annu. Rev. Plant Biol.* **54**: 265–306.
- Mikami, K., Katagiri, T., Iuchi, S., Yamaguchi-Shinozaki, K., and Shinozaki, K.** (1998). A gene encoding phosphatidylinositol-4-phosphatase 5-kinase is induced by water stress and abscisic acid in *Arabidopsis thaliana*. *Plant J.* **15**: 563–568.
- Molendijk, A.J., Bischoff, F., Rajendrakumar, C.S.V., Friml, J., Braun, M., Gilroy, S., and Palme, K.** (2001). *Arabidopsis thaliana* Rop GTPases are localized to tips of root hairs and control polar growth. *EMBO J.* **20**: 2779–2788.
- Mueller-Roeber, B., and Pical, C.** (2002). Inositol phospholipid metabolism in *Arabidopsis*. Characterized and putative isoforms of inositol phospholipid kinase and phosphoinositide-specific phospholipase C. *Plant Physiol.* **130**: 22–46.
- Munnik, T.** (2001). Phosphatidic acid: An emerging plant lipid second messenger. *Trends Plant Sci.* **6**: 227–233.
- Niggli, V.** (2005). Regulation of protein activities by phosphoinositide phosphates. *Annu. Rev. Cell Dev. Biol.* **21**: 57–79.
- Niwa, Y., Hirano, T., Yoshimoto, K., Shimizu, M., and Kobayashi, H.** (1999). Non-invasive quantitative detection and application of non-toxic, S65T-type green fluorescent protein in living plants. *Plant J.* **18**: 455–463.
- Ohashi, Y., Oka, A., Rodrigues-Pousada, R., Possenti, M., Ruberti, I., Morelli, G., and Aoyama, T.** (2003). Modulation of phospholipid

- signaling by GLABRA2 in root-hair pattern formation. *Science* **300**: 1427–1430.
- Olsen, H.L., et al.** (2003). Phosphatidylinositol 4-kinase serves as a metabolic sensor and regulates priming of secretory granules in pancreatic β cells. *Proc. Natl. Acad. Sci. USA* **100**: 5187–5192.
- Oude Weernink, P.A., Lopez de Jesus, M., and Schmidt, M.** (2007). Phospholipase D signaling: Orchestration by PIP₂ and small GTPases. *Naunyn Schmiedebergs Arch. Pharmacol.* **374**: 399–411.
- Oude Weernink, P.A., Schmidt, M., and Jakobs, K.H.** (2004). Regulation and cellular roles of phosphoinositide 5-kinases. *Eur. J. Pharmacol.* **500**: 87–99.
- Perera, I.Y., Davis, A.J., Galanopoulou, D., Im, Y.J., and Boss, W.F.** (2005). Characterization and comparative analysis of *Arabidopsis* phosphatidylinositol phosphate 5-kinase 10 reveals differences in *Arabidopsis* and human phosphatidylinositol phosphate kinases. *FEBS Lett.* **579**: 3427–3432.
- Peterson, R.L., and Farquhar, M.L.** (1996). Root hairs: Specialized tubular cells extending root surfaces. *Bot. Rev.* **62**: 2–33.
- Preuss, M.L., Schmitz, A.J., Thole, J.M., Bonner, H.K.S., Otegui, M.S., and Nielsen, E.** (2006). A role for the RabA4b effector protein PI-4K β 1 in polarized expansion of root hair cells in *Arabidopsis thaliana*. *J. Cell Biol.* **172**: 991–998.
- Qin, C., and Wang, X.** (2002). The *Arabidopsis* phospholipase D family. Characterization of a calcium-independent and phosphatidylcholine-selective PLD ζ 1 with distinct regulatory domains. *Plant Physiol.* **128**: 1057–1068.
- Ridge, R.W., and Emons, A.M.C.** (2000). *Root Hairs: Cell and Molecular Biology*. (Tokyo: Springer-Verlag).
- Ryan, E., Steer, M., and Dolan, L.** (2001). Cell biology and genetics of root hair formation in *Arabidopsis thaliana*. *Protoplasma* **215**: 140–149.
- Santarius, M., Lee, C.H., and Anderson, R.A.** (2006). Supervised membrane swimming: Small G-protein lifeguards regulate PIPK signalling and monitor intracellular PtdIns(4,5)P₂ pools. *Biochem. J.* **398**: 1–13.
- Smith, L.G., and Oppenheimer, D.G.** (2005). Spatial control of cell expansion by the plant cytoskeleton. *Annu. Rev. Cell Dev. Biol.* **21**: 271–295.
- Takehima, H., Komazaki, S., Nishi, M., Iino, M., and Kangawa, K.** (2000). Junctophilins: A novel family of junctional membrane complex proteins. *Mol. Cell* **6**: 11–22.
- Testerink, C., and Munnik, T.** (2005). Phosphatidic acid: A multifunctional stress signaling lipid in plants. *Trends Plant Sci.* **10**: 368–375.
- van Leeuwen, W., Okresz, L., Bogre, L., and Munnik, T.** (2004). Learning the lipid language of plant signalling. *Trends Plant Sci.* **9**: 378–384.
- van Leeuwen, W., Vermeer, J.E.M., Gadella, T.W.J., Jr., and Munnik, T.** (2007). Visualization of phosphatidylinositol 4,5-bisphosphate in the plasma membrane of suspension-cultured tobacco BY-2 cells and whole *Arabidopsis* seedlings. *Plant J.* **52**: 1014–1026.
- Vincent, P., Chua, M., Nogue, F., Fairbrother, A., Mekeel, H., Xu, Y., Allen, N., Bibikova, T.N., Gilroy, S., and Bankaitis, V.A.** (2005). A Sec 14p-nodulin domain phosphatidylinositol transfer protein polarizes membrane growth of *Arabidopsis thaliana* root hairs. *J. Cell Biol.* **168**: 801–812.
- Wang, X., Devaiah, S.P., Zhang, W., and Welti, R.** (2006). Signaling functions of phosphatidic acid. *Prog. Lipid Res.* **45**: 250–278.
- Westergren, T., Dove, S.K., Sommarin, M., and Pical, C.** (2001). AtPIP5K1, an *Arabidopsis thaliana* phosphatidylinositol phosphate kinase, synthesizes PtdIns(3,4)P₂ and PtdIns(4,5)P₂ *in vitro* and is inhibited by phosphorylation. *Biochem. J.* **359**: 583–589.
- Yin, H.L., and Janmey, P.A.** (2003). Phosphoinositide regulation of the actin cytoskeleton. *Annu. Rev. Physiol.* **65**: 761–789.
- Zonia, L., and Munnik, T.** (2006). Cracking the green paradigm: Functional coding of phosphoinositide signals in plant stress responses. *Subcell. Biochem.* **39**: 207–237.
- Zuo, J., Niu, Q.-W., and Chua, N.-H.** (2000). An estrogen receptor-based transactivator XVE mediates highly inducible gene expression in transgenic plants. *Plant J.* **24**: 265–273.